



Structural Global Performance Assessment Versus Individual Element-Oriented Performance-Based Assessment

Ebrahim Fadaei¹ · Hamzeh Shakib¹ · Alireza Azarbakht²

Received: 10 April 2018 / Accepted: 6 June 2019
© Shiraz University 2020

Abstract

In this paper, three new performance indices are proposed which can be used in order to determine the global performance of a given structure. The ASCE41-13 standard and the FEMA350 guidelines are used as representatives of, respectively, an element-oriented and a system-oriented performance-based assessment algorithm. Two ten-storeyed special steel moment frames, consisting of a regular and an irregular structure, are designed and assessed using these two algorithms. The results show that the element-oriented assessment algorithm significantly underestimates the seismic demand and capacity, especially in the case of the immediate occupancy and collapse prevention limit states. This underestimation can cause a significant drop in the estimated confidence levels.

Keywords Performance-based assessment · FEMA350 · ASCE41-13 · Confidence level

1 Introduction

Performance-based engineering (PBE) is a significant improvement in seismic design and assessment of buildings which has become increasingly used in recent decades. It aims to provide stakeholders with an interpretation of structural performance corresponding to a given hazard level (Bozorgnia and Bertero 2004).

FEMA356 was developed for the seismic rehabilitation of existing buildings. Four limit states have been introduced in FEMA356 (FEMA 2000a) which could be evaluated at different hazard levels by employing linear or nonlinear procedures. These limit states are: Immediate Occupancy (IO), Operational (O), Life Safety (LS), and Collapse Prevention (CP). FEMA356 later turned into ASCE41-06 (ASCE 2007) and ASCE41-13, which are mandatory regulations in the US. There is a shortcoming, however, which is that these regulations do not explicitly take into account either different uncertainties or acceptance criteria which are based on system-oriented behaviour. In the other word, exceeding a

limit state in just one structural element is interpreted as the whole structure has exceeded the prescribed global performance level.

The various structural limit states have mainly the same definitions in different regulations. For example, in ASCE41-13, IO corresponds to minor damage in which the structural system keeps its stiffness and strength without any residual drift. At the LS level, moderate damage occurs, but stiffness and strength change slightly. A residual drift will occur, and the structure needs to be repaired. At the CP level, the stiffness and strength change significantly, although the columns and walls of the building are still able to carry their gravity loads. Significant residual drift occurs, and the structure will be near collapse. No further occupancy of the structure is possible.

Incremental Dynamic Analysis (IDA) is a method involving comprehensive nonlinear response history analysis, which has been widely used in the last decade (Vamvatsikos and Cornell 2002). It can be used to define a given structural behaviour from elastic to extensively inelastic behaviour, by implementing an Engineering Demand Parameter (EDP) at different Intensity Measure (IM) values. The aleatory uncertainty is explicitly taken into account in the IDA procedure by including a relatively large set of ground motion records. Despite the excellent progress which has already been made within the IDA calculation method (Vamvatsikos and Cornell 2004, 2005, Han and Chopra 2006;

✉ Hamzeh Shakib
shakib@modares.ac.ir

¹ School of Civil and Environmental Engineering, Tarbiat Modares University, Tehran, Iran

² Department of Civil Engineering, Faculty of Engineering, Arak University, P.O. Box 38156-8-8349, Arāk, Iran

Vamvatsikos and Fragiadakis 2010; Dolsek 2009; Asgarian et al. 2010; Azarbakht and Dolšek 2011), the definitions of different limit states on an individual IDA curve still remain a practical challenge. This issue has different aspects in the case of different seismic lateral bearing systems. For example, the FEMA350 criteria are based on experimental data for steel moment frames, i.e. Liu and Astaneh-Asl (2000), Lee and Foutch (2000), Venti and Engelhardt (2000), Lee et al. (2000), and Gilton et al. (2000). The IO limit state which corresponds to the Maximum Inter-storey Drift Ratio (MIDR) reaches up to 2%. The CP limit state is reached if the MIDR reaches up to 10%, or if the IDA curve slope drops to a value which is less than 20% of the initial (elastic) stiffness. The global structural behaviour is used to define the limit states in the FEMA350 guideline (FEMA 2000b).

On the other hand, by the ASCE41-13 standard (ASCE/SEI 2014), a set of appropriate plastic hinges needs to be assigned to each element. The maximum deformation during the response history analysis is then compared to the acceptable thresholds (provided in the standard). Consequently, when the first element demand is exceeded, this is taken as the limit state of the structure. In other words, the ASCE41-13 standard implements an individual-element-oriented criterion in order to define this limit state.

When an element goes beyond the performance threshold, this does not necessarily mean that the whole structural limit state has been reached. This critical issue is addressed in the US Army Corp of Engineers' Manual: Earthquake design and evaluation of concrete hydraulic structures (USACE 2007), as well as in the FEMAP695 guideline (FEMA 2009). This issue is the main focus of the current study, where it has been assumed that the seismic design (or assessment) of a specific structure based on the two regulations should produce nearly the same result. For this reason, two ten-storeyed special steel moment frame structures are assessed by means of FEMA350, as being representative of the global behaviour point of view, as well as by ASCE41-13, as being representative of the element-oriented behaviour point of view. The number of elements, the cumulative time intervals of demand excess in hinges, the ratio of maximum hinge rotation to capacity rotation, and the global confidence levels are calculated and discussed in detail in order to propose a new viewpoint in this area of research.

2 Methodology

In order to assess the ASCE41-13 definitions for limit states, two ten-storeyed special steel moment frame structures have been designed based on the ASCE7-10 (ASCE 2010) and AISC (2010) regulations. The first structure is regular in all its aspects, whereas the second structure is irregular in height. IDA has been performed for the given structures for

a set of appropriate ground motion records. The EDP and IM corresponding to the IO and CP limit states have been defined on each IDA curve, based on the FEMA350 guideline. Three new indices are then proposed including: a Cumulative Time Demand Excess Ratio (CTDER), a Maximum Hinge Demand Excess Ratio (MHDER), and a Ratio of Demand Excess Elements (RDEE). The CTDER index is expressed mathematically as $CTDER_{i,k} = \frac{t_{ce,i}}{t_{d,k}}$ and is employed to determine the time ratio that demand in each of the plastic hinge of the structure is more than the intended limit state. In this relation i is the element number, k is the record number, $t_{ce,i}$ is the cumulative time for which the demand exceeds the acceptance level (based on ASCE41-13), and $t_{d,k}$ is the total ground motion significant duration (Trifunac and Brady 1975). This index is calculated for each hinge of a given element and a given ground motion. The total damage in each element will clearly increase as the CTDER index increases.

The MHDER index is defined as $MHDER_{i,k} = \frac{\theta_{max,i,k}}{\theta_{lim}}$, where $\theta_{max,i,k}$ is the maximum hinge rotation in the i th element in the case of the k th ground motion record. θ_{lim} is the acceptable hinge rotation based on the ASCE41-13 standard. It shows the magnitude of the demand excess in each hinge under the effect of a particular ground motion record. This index, too, apparently has a positive correlation with the total damage in each element.

The RDEE index, is defined as $RDEE_k = \frac{N_{ce,k}}{N_{el}}$, takes into account the normalised number of elements that are beyond the acceptance criteria based on the ASCE41-13 standard. In this equation N_{el} is the number of elements of beam or column distinctly, $N_{ce,k}$ is the number of elements that their demand exceeds the acceptance level (based on ASCE41-13).

It should be mentioned that in this study these indices were calculated for the columns and beams separately. The idea was that various combinations of these three proposed indices would shed light on the detailed behaviour of the structural system as a whole. This should make possible decisions about whether or not the assessment of a given structure as a whole is acceptable. This issue is discussed in detail in the following sections.

3 Structural Models and Analysis

The two investigated ten-storeyed special steel moment frames have been designed based on the provisions of AISC 2010 and are shown in Fig. 1. The first structure has no irregularities, whereas, in the second structure, the ratio of lateral stiffness at five bottom stories over the lateral stiffness of the sixth story is 0.6, hence according to ASCE 7-10, it has extreme soft story irregularity along the height. Both

Fig. 1 Properties of the designed structures in this study, **a** plan view and **b** elevation view

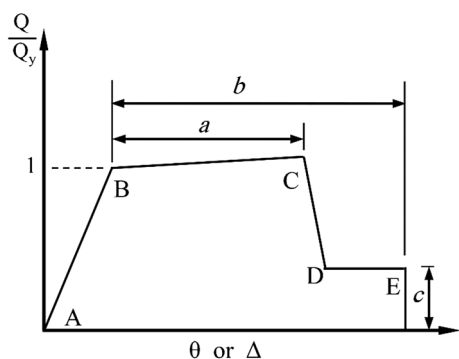
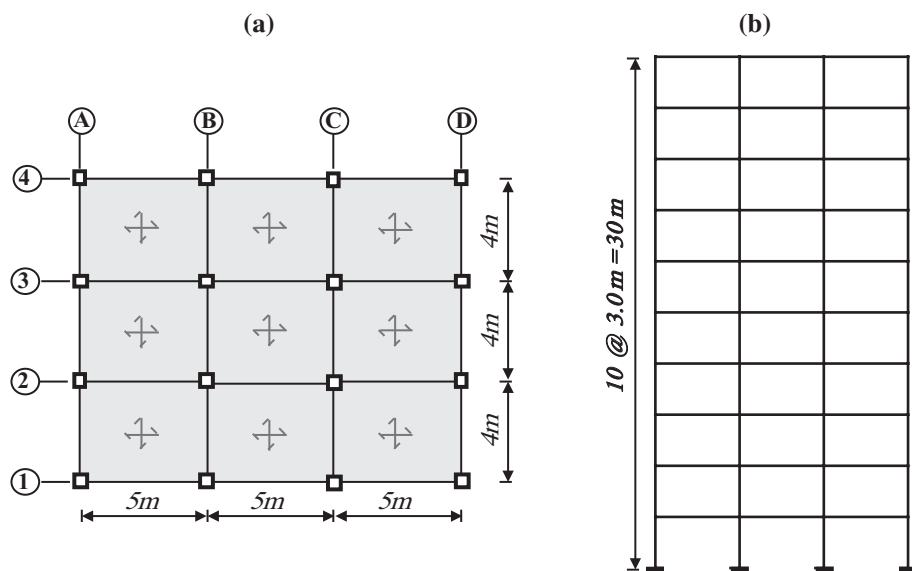


Fig. 2 The schematic nonlinear backbone for beam and column members (ASCE/SEI 2014)

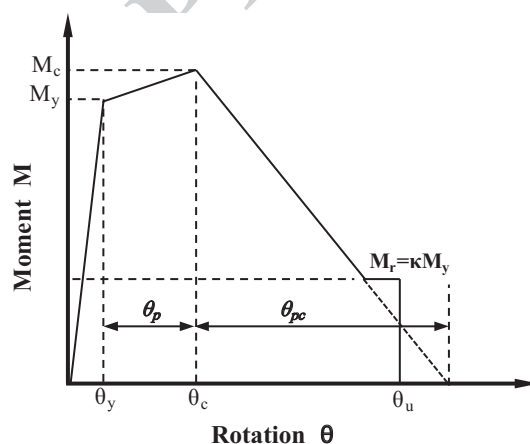


Fig. 3 The Ibarra-Krawinkler backbone deterioration model (Ibarra and Krawinkler 2005)

161 structures were designed for a highly seismic region, i.e. the
 162 Tehran metropolis, and soil type C (based on the ASCE7-10
 163 standard). The dead and live loads on the typical floors are,
 164 respectively, equal to 600 kg/m² and 200 kg/m². Rectangular
 165 box-shaped and IPE profiles have been used for the column
 166 and beam sections, respectively. To make stiffness irregularity,
 167 Young's modulus of the material of the members of the
 168 lateral resisting system at the bottom half stories of the structure
 169 was changed. The effective mass and lateral strength are
 170 identical for both structures, and their fundamental period
 171 is equal to 1.37 s.

172 The OpenSees platform has been utilised in order to perform
 173 the nonlinear analyses (*OpenSees*). In order to simplify the
 174 analysis procedure, a 2D model has been created. Elastic beam-column
 175 elements with two nonlinear zero-length elements, at each of the two
 176 ends, have been used to model the beams and columns. The nonlinear
 177 backbone curve is defined based on the ASCE41-13 standard (ASCE/
 178 SEI 2014) and is shown schematically in Fig. 2. The strain
 179

hardening part, marked as the lines B and C in Fig. 2, has a
 slope which is equal to 3% of the initial (elastic) slope. The
 Ibarra and Krawinkler model (Ibarra and Krawinkler 2005)
 has been implemented within the OpenSees platform; it consists
 of five modelling parameters, as shown in Fig. 3. The five
 modelling parameters include: (1) the pre-capping plastic rotation,
 θ_p (2) the post-capping (i.e. from maximum moment to fracture)
 plastic rotation, θ_{pc} (3) the cumulative rotation capacity that
 determines the reference energy dissipation capacity of a structural
 component, Λ (4) the effective-to-predicted component yield
 strength, M_y/M_{yp} and (5) the capping-strength-to-effective-yield-
 strength ratio, M_c/M_y .

Rayleigh damping proportional to mass and stiffness (Chopra 1995)
 has been assumed by considering 5% damping for the first and
 third modes. The stiffness matrix at

the current state is employed to construct the stiffness-proportional term of damping matrix. The floors have been assumed to be rigid, and the P-Delta effect has been taken into consideration (Mazzoni et al. 2003).

The Hunt and Fill algorithm (Vamvatsikos and Cornell 2004) is utilised within the IDA algorithm in order to quantify the structural limit states in terms of IM and EDP. The spectral acceleration at the fundamental period of structure and 5% damping, $S_a(T1, 5\%)$ is taken as the IM measure, and the MIDR is assumed as the EDP. It is worth noting that MIDR has a positive correlation with the structure's global instability, as well as with the limit states (FEMA 2000b). A total of 44 far-field ground motion records were used as input for the IDA. These records were extracted from the specified far-field ground motion record set of FEMA P695 (FEMA 2009) that includes 22 component pairs of horizontal ground-motions. The moment magnitude of the given records was between 6.5 and 7.6, and no directivity effect can be observed among them. The characteristics of the records are summarised in Table 1.

4 Limit States Definitions

In this section, the seismic performance is assessed by three algorithms, as follows:

The IO and CP limit states are controlled by implementing the FEMA350 and ASCE41-13 algorithms, respectively, as being representative of system-oriented and element-oriented behaviours. As already mentioned, in FEMA350 these performance levels are determined based on MIDR and in ASCE41-13 according to deformation demands of plastic hinges is determined.

1. CTDER, MHDER and RDEE indices are employed in order to combine the element-oriented and the system-oriented point of views. This should help to define the structure's behaviour as a whole.
2. The confidence levels, at the IO and CP limit states, are calculated based on the element-oriented and system-oriented point of views.

4.1 Element-Oriented and System-Oriented Limit States

As all the parameters were identical for the structural analysis, it was anticipated that the limit states would be relatively close, based on the FEMA350 and ASCE41-13 algorithms.

The IO and CP limit states on the median IDA curve are shown in Fig. 4 in the case of the FEMA350 and ASCE41-13 algorithms. As can be clearly seen from this figure, the two algorithms mentioned above do not result in nearly the same points for the IO and CP limit states. Based on the

element-oriented assessment algorithm (ASCE41-13) the structures exceed the performance levels at less IMs when compared to the system-oriented assessment algorithm (FEMA350), thus in determining the performance levels, the element-oriented approach is more conservative. To further investigate this issue, the differences between the IMs, in the cases of the IO and CP limit states, respectively, versus the ground motion records are shown in Figs. 5 and 6, from which it can be seen that these differences are more significant in the case of the IO than in the case of the CP limit state. Although this study was not focussed on irregularity effects, it can also be clearly seen from Figs. 5 and 6 that the differences are more significant in the case of the irregular structure when compared with the regular structure. On average, the difference between the IMs corresponding to the element-oriented and system-oriented algorithms, were, respectively, 67% and 44%, in the case of the IO and CP limit states. This issue is further elaborated in the following sections.

4.2 Limit States Based On the Newly Proposed Indices

In the element-oriented assessment algorithm, any hinge demand excess corresponds to a structural limit state. However, no information about the size of this demand excess is available. In other words, the cumulative amount of demand excess in individual hinges has to reach a certain level in order to be able to degrade the total stiffness and strength of the structure sufficiently. The IMs corresponding to the IO and CP limit states, based on the FEMA350 guidelines, are taken here as benchmarks since the FEMA350 recommendations are based on extensive experimental data, e.g. see Liu and Astaneh-Asl (2000), Lee and Foutch (2000), Venti and Engelhardt (2000) and Gilton et al. (2000). The CTDER, MHDER and RDEE indices are then calculated independently for the beams and columns. For example, the CTDER index shown in Fig. 7 corresponds to an IO limit state based on the ASCE41-13 standard in the case of the regular structure under the effect of record No. 1. As can be seen in Fig. 7, the majority of the beam elements are beyond the IO limit state, for at least more than 20% of the ground motion significant duration. The CTDER index is averaged over the whole beam hinges, which presents a 38.5% data point in Fig. 8. In fact, Fig. 8 shows the average CTDER index versus the different ground motion records. As can be seen from this figure, most of the beams show nonlinear behaviour beyond the limit state, although this varies between 8 and 66%, depending on the input ground motion. Figure 9 shows the average MHDER index, only over the demand for excess elements. This index is up to three and four, respectively, in the cases of both the regular

Table 1 Characteristics of the 44 ground motion records for the IDA analysis (FEMA 2009)

No.	Event	Station	Magnitude	Distance (km)	PGA (g)	Time duration (s)
1	Kobe, Japan, 1995	Nishi-Akashi, 090	6.9	25.2	0.5	11.25
2	Kobe, Japan, 1995	Shin-Osaka, 000	6.9	28.5	0.24	10.35
3	Kocaeli, Turkey, 1999	Arcelik, 000	7.5	13.5	0.22	11.06
4	San Fernando, 1971	LA-Hollywood Stor FF, 090	6.6	25.9	0.21	13.17
5	Landers, 1992	Coolwater, LN	7.3	20	0.28	10.58
6	Landers, 1992	Coolwater, TR	7.3	20	0.42	8.24
7	Superstition Hills, 1987	Poe Road (temp), 270	6.5	11.7	0.45	13.71
8	Superstition Hills, 1987	Poe Road (temp), 360	6.5	11.7	0.3	13.66
9	Hector Mine, 1999	Hector, 000	7.1	12	0.27	11.68
10	Manjil, Iran, 1990	Abbar, T	7.4	13	0.5	29.12
11	Chi-Chi, Taiwan, 1999	TCU045, E	7.6	26.8	0.47	11.34
12	Chi-Chi, Taiwan, 1999	TCU045, N	7.6	26.8	0.51	10.82
13	Friuli, Italy, 1976	Tolmezzo, 000	6.5	15.8	0.35	4.25
14	Landers, 1992	Yermo Fire Station, 270	7.3	23.8	0.24	17.6
15	Landers, 1992	Yermo Fire Station, 360	7.3	23.8	0.15	18.88
16	Loma Prieta, 1989	Gilroy Array #3, 000	6.9	12.8	0.56	6.37
17	Northridge, 1994	W Lost Cany, 000	6.7	12.4	0.41	6.29
18	Northridge, 1994	W Lost Cany, 270	6.7	12.4	0.48	5.58
19	San Fernando, 1971	LA—Hollywood Stor FF, 180	6.6	25.9	0.17	13.43
20	Kocaeli, Turkey, 1999	Duzce, 180	7.5	15.4	0.31	11.80
21	Kocaeli, Turkey, 1999	Duzce, 270	7.5	15.4	0.36	10.86
22	Loma Prieta, 1989	Capitola, 000	6.9	35.5	0.53	12.15
23	Loma Prieta, 1989	Capitola, 090	6.9	35.5	0.44	13.16
24	Imperial Valley, 1979	Delta, 262	6.5	22.5	0.24	51.43
25	Imperial Valley, 1979	Delta, 352	6.5	22.5	0.35	50.52
26	Northridge, 1994	Beverly Hills-14,145 Mulhol, 009	6.7	17.15	0.44	9.26
27	Northridge, 1994	Beverly Hills-14,145 Mulhol, 279	6.7	17.15	0.52	8.15
28	Duzce_ Turkey, 1999	Bolu. 000	7.14	12.04	0.82	8.55
29	Duzce_ Turkey, 1999	Bolu. 090	7.14	12.04	0.8	9.02
30	Imperial Valley, 1979	El Centro Array #11, 140	6.5	12.56	0.37	9.0
31	Imperial Valley, 1979	El Centro Array #11, 230	6.5	12.56	0.38	7.94
32	Kobe, Japan, 1995	Nishi-Akashi, 000	6.9	25.2	0.48	9.60
33	Kobe, Japan, 1995	Shin-Osaka, 090	6.9	28.5	0.23	11.60
34	Kocaeli, Turkey, 1999	Arcelik, 090	7.5	13.5	0.13	10.23
35	Loma Prieta, 1989	Gilroy Array #3, 090	6.9	12.8	0.37	11.37
36	Manjil, Iran, 1990	Abbar, L	7.4	13	0.51	28.66
37	Superstition Hills, 1987	El Centro Imp. Co. Cent, 000	6.5	18.2	0.36	28.0
38	Superstition Hills, 1987	El Centro Imp. Co. Cent, 090	6.5	18.2	0.26	35.7
39	Hector Mine, 1999	Hector, 090	7.1	12	0.33	9.65
40	Friuli, Italy, 1976	Tolmezzo, 270	6.5	15.8	0.32	4.92
41	Chi-Chi, Taiwan, 1999	CHY101, E	7.6	9.94	0.34	30.3
42	Chi-Chi, Taiwan, 1999	CHY101, N	7.6	9.94	0.44	26.5
43	Cape Mendocino	Shelter Cove Airport, 000	7.01	28.78	0.23	16.08
44	Cape Mendocino	Shelter Cove Airport, 090	7.01	28.78	0.18	17.52

293 and the irregular structure. By averaging over the records,
294 the CTDER index is 38.5%, and the MHDER index is 2.65.

295 The RDEE index is shown in Fig. 10, which confirms
296 that almost 89% of the beams have gone beyond their limit

states. On the other hand, no column had any demand excess
at the IO limit state. A summary of the behaviour of the
two investigated structures, referring to the IO limit state, is
provided in Table 2.

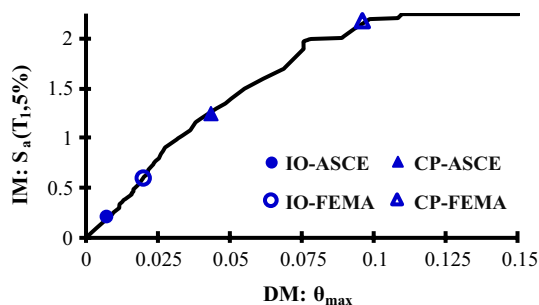


Fig. 4 The IO and LS limit states on the median IDA curve of the regular structure obtained on the basis of the FEMA350 and ASCE41-13 regulations

Fig. 5 The difference between the IMs corresponding to the IO limit state versus the ground motion records based on the FEMA350 and ASCE41-13 algorithms

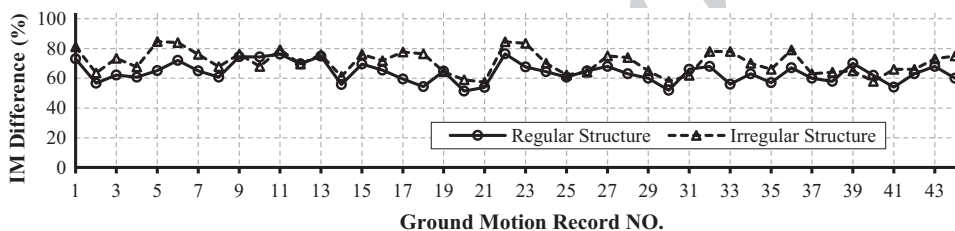


Fig. 6 The difference between the IMs corresponding to the CP limit state versus the ground motion records based on the FEMA350 and ASCE41-13 algorithms

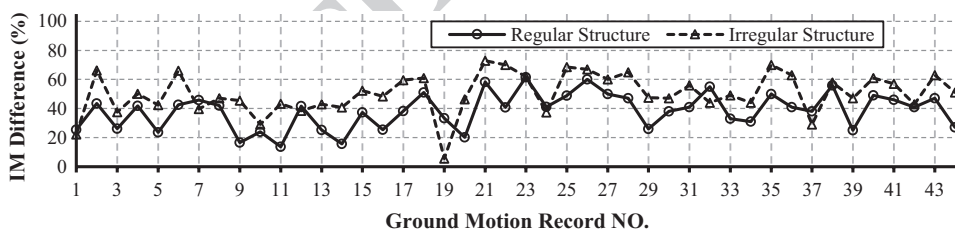


Fig. 7 The CTDER index versus different beam elements at an IM corresponding to the IO limit state based on ASCE41-13, and the regular structure, under record No.1

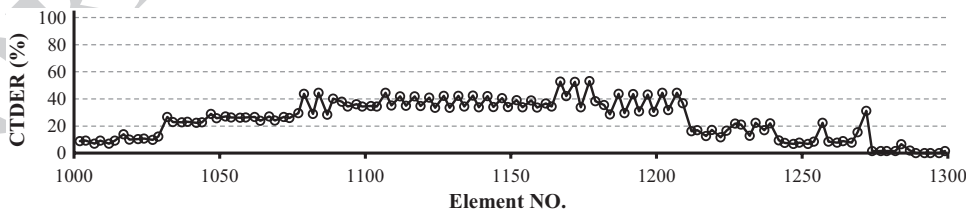
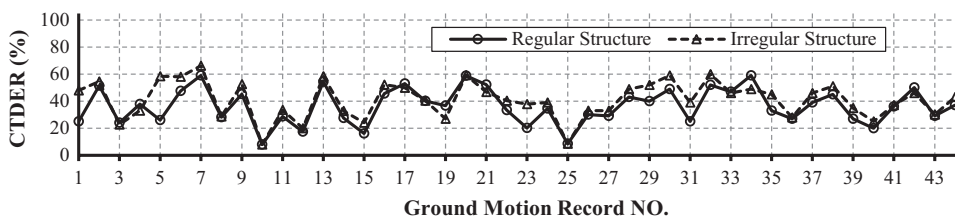


Fig. 8 The beams' average CTDER index versus the different ground motion records in the case of the IO limit state based on ASCE41-13



the MHDR index is 1.58. In addition, 61% of the beams experience a certain level of demand excess.

In the case of the IM corresponding to the CP limit state (based on FEMA350), only the demand at the bottom of the first storey columns exceeds the limit state (based on ASCE41-13). This behaviour was anticipated, since columns are usually designed more conservatively than beams, especially in special moment frames. The average values of the CTDER and MHDR indices are shown, respectively, in Figs. 14 and 15, in the case of the first storey columns. It is worth mentioning that, as shown in Fig. 15, the absence of MHDR in some records means that the deformation demand at the bottom of the first story columns under the effect of that records has not exceeded the CP limit state. By

305
306
307
308
309
310
311
312
313
314
315
316
317
318

301 The average values of the CTDER and MHDR indices, and the RDEE indices for the beams are presented, for
302 the CP limit state, in Figs. 11, 12 and 13, respectively. By
303 averaging over the records, the CTDER index is 13%, and
304

319 averaging over the records, the CTDER index is 14.5%, and
320 the MHDR index is 1.54. A summary referring to the CP
321 limit state is provided in Table 3.

Fig. 9 The beams' average MHDR index versus the different ground motion records in the case of the IO limit state based on ASCE41-13

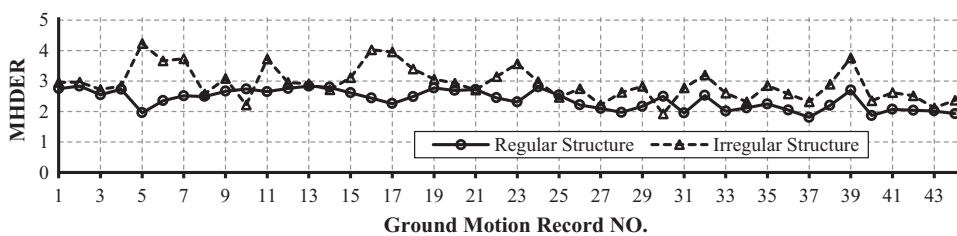


Fig. 10 The beams' RDEE index versus the different ground motion records in the case of the IO limit state based on ASCE41-13

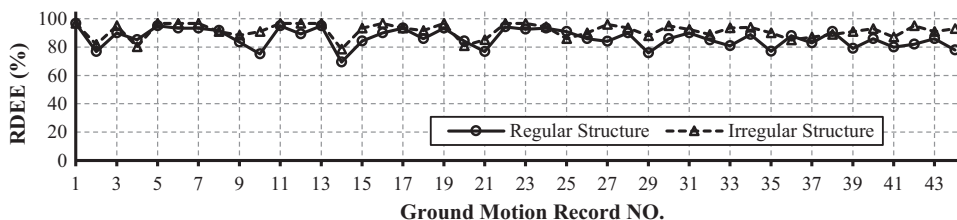


Table 2 Summary of the proposed indices for the given structures at the IO limit state

Structural members	Beams		Columns	
	Regular	Irregular	Regular	Irregular
CTDER	36%	40%	0	0
RDEE	86%	91%	0	0
MHDR	2.4	2.9	0	0

4.3 Confidence Levels

322

The confidence level is a level of confidence in the ability of building to meet any desired performance objectives that is a measure of the accuracy and reliability to design with considering uncertainty in determination structural demands and capacities.

323

324

325

326

327

Evaluation of the structural confidence level at a specific performance objective has been accomplished in the

328

329

Fig. 11 The average CTDER index for the beams versus the different ground motion records, in the case of the CP limit state based on ASCE41-13

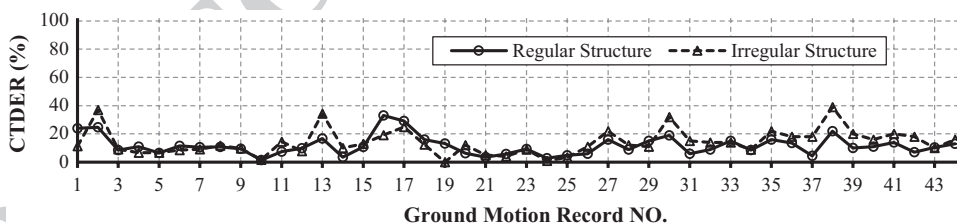


Fig. 12 The average MHDR index for the beams, versus the different ground motion records, in the case of the CP limit state based on ASCE41-13

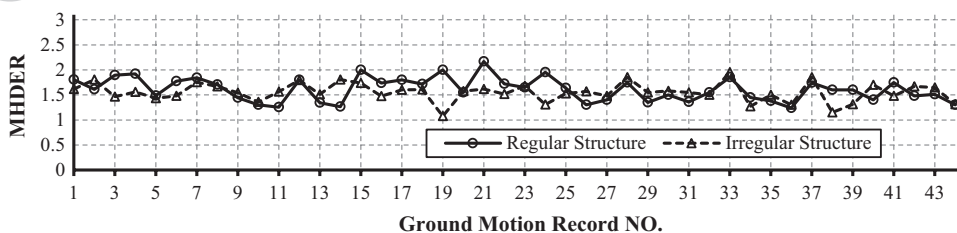
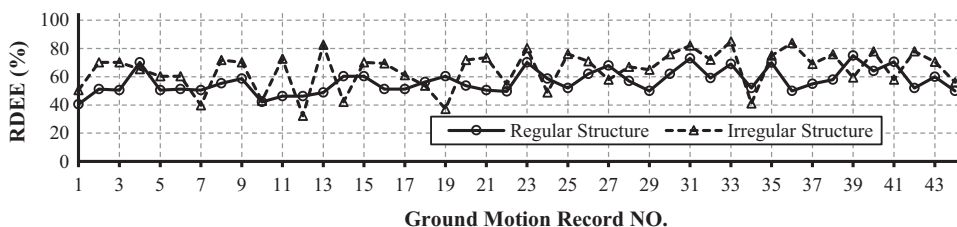


Fig. 13 The RDEE index for the beams, versus the different ground motion records, in the case of the CP limit state based on ASCE41-13



Author Proof

Fig. 14 The average CTDER index for the first storey columns, versus the different ground motion records, in the case of the CP limit state

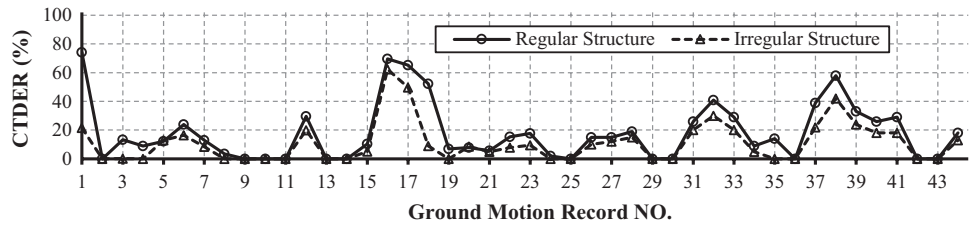


Fig. 15 The average MHDR index for the first storey columns, versus the different ground motion records, in the case of the CP limit state

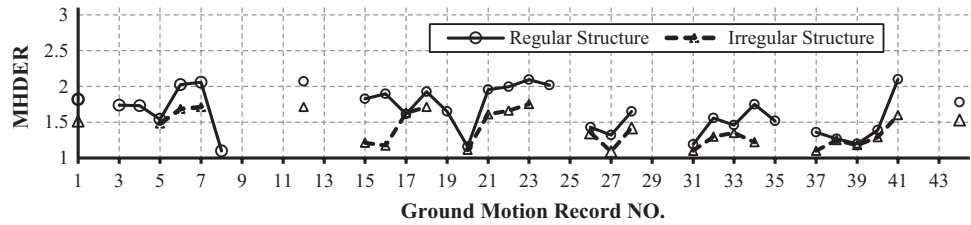


Table 3 Summary of the proposed indices for the given structures at the CP limit state

Structural members	Beams		Base of columns	
	Regular	Irregular	Regular	Irregular
CTDER	12%	14%	18%	11%
RDEE	57%	65%	72%	65%
MHDR	1.61	1.55	1.66	1.41

where

$$\beta_{UT} = \sqrt{\beta_{UD}^2 + \beta_{UC}^2} \tag{2}$$

$$\gamma_R = \text{EXP}\left(\frac{k}{2b}\beta_{RD}^2\right) \tag{3}$$

$$\phi_R = \text{EXP}\left(-\frac{k}{2b}\beta_{RC}^2\right) \tag{4}$$

framework of the reliability-based probabilistic approach (Cornell et al. 2002), which incorporates randomness and uncertainty of both the seismic loading and the structural resistance in the analysis procedure.

One set of factors increases the demand whereas another set of factors decreases the capacity in order to account for different uncertainties as well as different regional seismicity characteristics. The seismic demand is calculated by taking into account the Tehran metropolis, with $k=4.07$ and $b=1.0$, where k is the logarithmic slope of the hazard curve, and b is a coefficient which relates the incremental change in demand to an incremental change in ground shaking intensity, at the hazard level of interest, typically taken as having a value of 1.0 (Cornell et al. 2002). On the other hand, the capacity is obtained based on (1) FEMA350 by applying the previously mentioned rules on the IDA curves, and (2) ASCE41-13 by monitoring the first hinge which shows a demand excess beyond the limit state. The confidence level can be obtained based on the standard Gaussian variate associated with the probability x of not being exceeded, K_x , which is calculated as follows:

$$\text{EXP}(-\beta_{UT}K_x) = \frac{\gamma_R D}{\phi_R C} = \lambda_x \tag{1}$$

In these equations, C is the median drift capacity, D is the median drift demand (determined from the IDA procedure), ϕ_R is the resistance factor for considering the randomness inherent in the prediction of the capacity of the structure as a function of ground shaking, and γ_R is the demand variability factor. Here, β_{RC} and β_{RD} are the standard deviation of the natural logarithms of the drift capacity and demand, respectively. Additionally, β_{UC} and β_{UD} are uncertainty factors involved in the estimation of the capacity and demand, which are caused by limited knowledge and data on the design or nonlinear structural modelling and other approximations.

A summary of confidence levels for the different structures and different algorithms is given in Table 4, from which it can be seen that all the confidence levels are above 96% except in the case of the IO limit state when using the ASCE41-13 regulations. Recalling the Cornell method, the parameter λ is equal to the ratio of the factored demand over the factored capacity. Additionally, based on the standard Gaussian distribution, $\lambda=0.86$ is identical to a 90% confidence level, and lower λ values will achieve higher values of the confidence level. In other words, as can be seen in Table 4, all the λ values are below 0.86 except in the case of the IO limit state when using the

Author Proof

Table 4 Confidence levels for the IO and CP limit states, based on the FEMA350 and the ASCE41-13 regulations

Performance objective	Structure	Capacity calculation algorithm	S_a (T1, 5%)	D	γ	γ_a	C	ϕ	λ	K_x	CL (%)
IO limit state against the 50/50 hazard level	Regular	FEMA350	0.2g	0.0076	1.20	1.035	0.0200	1	0.472	5.31	> 99.7
		ASCE41-13	0.2g	0.0076	1.20	1.035	0.0078	0.9872	1.232	-1.08	13.90
	Irregular	FEMA350	0.2g	0.0067	1.05	1.035	0.0200	1	0.365	7.03	> 99.7
		ASCE41-13	0.2g	0.0067	1.05	1.035	0.0059	0.9329	1.306	-1.47	7.02
CP limit state against the 2/50 hazard level	Regular	FEMA350	0.47g	0.0171	1.15	1.085	0.0910	0.8823	0.265	4.13	> 99.7
		ASCE41-13	0.47g	0.0171	1.15	1.085	0.0437	0.9209	0.530	2.40	99.19
	Irregular	FEMA350	0.47g	0.0159	1.11	1.085	0.0863	0.8222	0.269	4.10	> 99.7
		ASCE41-13	0.47g	0.0159	1.11	1.085	0.0332	0.8288	0.692	1.73	96.86

D median structural demand, C median structural capacity, γ demand variability factor, γ_a analysis uncertainty factor, ϕ resistance factor, λ confidence parameter, K_x standard Gaussian variate associated with the probability x of not being exceeded, CL confidence level

ASCE41-13 regulations, in which the parameter λ is equal to 1.232 and 1.306 in the case of both the regular and the regular structure, respectively. These values of λ result in confidence levels lesser than 14%, which is not acceptable for design purposes. As these structures were designed based on up-to-date design standards, this is proof that the ASCE41-13 standard significantly underestimates the capacity corresponding to the IO limit state. Although the capacity estimates are entirely different in the case of the CP limit state, nevertheless the confidence levels are above 96% in the case of both the FEMA350 and the ASCE41-13 standards.

5 Conclusions

In this study, the performance-based assessment was investigated from two different points of views, as follows: (1) the FEMA350 guidelines, being a representative of system-oriented behaviour, and (2) the ASCE41-13 standard, being a representative of element-oriented behaviour. These regulations assessed two regular and irregular structures, and Immediate Occupancy and Collapse Prevention limit states were defined. Additionally, three new indices are proposed in order to justify the differences between the results obtained by using these two different algorithms. The results show that the element-oriented algorithm significantly underestimates the seismic capacity in the case of both the IO and the CP limit states. However, this underestimation results in a reduction of the confidence level, especially in the case of the IO limit state.

At the IO limit state, and based on the FEMA350 regulations, over 89% of the beams experience a demand excess beyond the acceptable level. These beams stay, on average, above the acceptable threshold for 38.5% of the motion duration. On average, the plastic rotation in these beams goes up to 260% beyond the acceptable threshold. On the other hand, no columns experience any demand excess at this limit state.

At the CP limit state, and based on the FEMA350 regulations, over 61% of the beams experience a demand excess beyond the acceptable level. These beams stay, on average, above the acceptable threshold for 13% of the motion duration. On average, the plastic rotation in these beams goes up to 58% beyond the acceptable threshold. On the other hand, at their bases, all the first storey columns experience a demand excess in the case of the majority of the used ground motion records. The demand excess in the first storey columns, on average in 14.5% of the motion duration, reaches up to 53% beyond the acceptable level.

In summary, the element-oriented algorithm significantly underestimates the seismic demand when compared to the system-oriented algorithm. It should be mentioned that the results presented in this paper are limited by the assumptions

434 made and that further investigations are necessary to shed
435 more light on this critical line of research.

436 References

- 437 AISC (2010) Specification for structural steel buildings. ANSI/AISC
438 360-10, Chicago
- 439 ASCE (2007) Seismic rehabilitation of existing buildings. ASCE/SEI
440 41-06, Reston, VA
- 441 ASCE (2010) Minimum design loads for buildings and other structures.
442 ASCE/SEI 7-10, Reston, VA
- 443 ASCE/SEI (Structural Engineering Institute) (2014) Seismic evaluation
444 and retrofit of existing buildings. ASCE/SEI 41-13, Reston, VA
- 445 Asgarian B, Sadrinezhad A, Alanjari P (2010) Seismic performance
446 evaluation of steel moment resisting frames through incremental
447 dynamic analysis. *J Constr Steel Res* 66(2):178–190
- 448 Azarbakht A, Dolšek M (2011) Progressive incremental dynamic anal-
449 ysis for first-mode dominated structures. *J Struct Eng* 137:445–
450 455. [https://doi.org/10.1061/\(ASCE\)ST.1943-541X.0000282](https://doi.org/10.1061/(ASCE)ST.1943-541X.0000282)
- 451 Bozorgnia Y, Bertero VV (eds) (2004) Earthquake engineering. CRC
452 Press, New York
- 453 Chopra AK (1995) Dynamics of structures: theory and applications to
454 earthquake engineering. Prentice-Hall, Inc., Upper Saddle River
- 455 Cornell CA, Jalayer F, Hamburger RO, Foutch DA (2002) The proba-
456 bilistic basis for the 2000 SAC/FEMA steel moment frame guide-
457 lines. *ASCE J Struct Eng* 128(4):526–533
- 458 Dolšek M (2009) Incremental dynamic analysis with consideration of
459 modeling uncertainties. *Earthq Eng Struct Dyn* 38(6):805–825
- 460 FEMA (2000a) Prestandard and commentary for the seismic rehabilita-
461 tion of buildings. FEMA-356, Washington, DC
- 462 FEMA (2000b) Recommended seismic design criteria for new steel
463 moment frame buildings. Report No. FEMA-350, SAC Joint Ven-
464 ture, Federal Emergency Management Agency, Washington, DC
- 465 FEMA (2009) Quantification of building seismic performance factors.
466 Rep. FEMA-P695, FEMA, Washington, DC
- 467 Gilton C, Chi B, Uang CM (2000) Cyclic testing of a free flange
468 moment connection. SAC/BD-00/19, SAC Joint Venture, Sacra-
469 mento, CA
- Han WW, Chopra AK (2006) Approximate incremental dynamic anal-
470 ysis using the modal pushover analysis procedure. *Earthq Eng*
471 *Struct Dyn* 35(15):1853–1873
- Ibarra LF, Krawinkler H (2005) Global collapse of frame structures
472 under seismic excitations. Report No. TB 152, The John A. Blume
473 Earthquake Engineering Center, Stanford Univ., Stanford, CA
474
- Lee K, Foutch DA (2000) Performance prediction and evaluation of
475 steel special moment frames for seismic loads. SAC Background
476 Document SAC/BD-00/25, SAC Joint Venture, Richmond, CA
477
- Lee K-H, Stojadinovic B, Goel SC, Margarian AG, Choi J, Wongkaew
478 A, Reyher B P, Lee D-Y (2000) Parametric tests on unreinforced
479 connections. SAC Background Document SAC/BD-00/01, SAC
480 Joint Venture, Richmond, CA
481
- Liu J, Astaneh-Asl A (2000) Cyclic tests on simple connections
482 including effects of the slab. SAC Background Document SAC/
483 BD-00/03, SAC Joint Venture, Richmond, CA
484
- Mazzoni S, McKenna F, Scott MH, Fenves GL, Jeremic B (2003)
485 OpenSees command language manual. Pacific Earthquake Engi-
486 neering Research Center. University of California, Berkeley
487
- OpenSees [Computer software]. Berkeley, CA, University of California
488
- Trifunac MD, Brady AG (1975) A study on the duration of strong
489 earthquake ground motion. *Bull Seismol Soc Am* 65(3):581–626
490
- USACE (U.S. Army Corps of Engineers) (2007) Earthquake design
491 and evaluation of concrete hydraulic structures. Report No. EM
492 1110-2-6053, Dept. of the Army, Washington, DC
493
- Vamvatsikos D, Cornell CA (2002) Incremental dynamic analysis.
494 *Earthq Eng Struct Dyn* 31(3):491–514
495
- Vamvatsikos D, Cornell CA (2004) Applied incremental dynamic
496 analysis. *Earthq Spectra* 20(2):523–553
497
- Vamvatsikos D, Cornell CA (2005) Direct estimation of seismic
498 demand and capacity of multidegree-of-freedom systems through
499 incremental dynamic analysis of single degree of freedom approx-
500 imation. *J Struct Eng* 131:589–599. [https://doi.org/10.1061/\(ASCE\)0733-9445\(2005\)131:4\(589\)](https://doi.org/10.1061/(ASCE)0733-9445(2005)131:4(589))
501
- Vamvatsikos D, Fragiadakis M (2010) Incremental dynamic analysis
502 for estimating seismic performance sensitivity and uncertainty.
503 *Earthq Eng Struct Dyn* 39(2):141–163
504
- Venti M, Engelhardt MD (2000) Test of a free flange connection
505 with a composite floor slab. SAC Background Document SAC/
506 BD-00/18, SAC Joint Venture, Richmond, CA
507

